Power-over-Skin: Full-Body Wearables Powered By Intra-Body RF Energy

Andy Kong
Carnegie Mellon University
Pittsburgh, USA

Daehwa Kim
Carnegie Mellon University
Pittsburgh, USA

Chris Harrison
Carnegie Mellon University
Pittsburgh, USA

ABSTRACT

Powerful computing devices are now small enough to be easily worn on the body. However, batteries pose a major design and user experience obstacle, adding weight and volume, and generally requiring periodic device removal and recharging. In response, we developed Power-over-Skin, an approach using the human body itself to deliver power to many distributed, battery-free, worn devices. We demonstrate power delivery from on-body distances as far as from head-to-toe, with sufficient energy to power microcontrollers capable of sensing and wireless communication. We share results from a study campaign that informed our implementation, as well as experiments that validate our final system. We conclude with several demonstration devices, ranging from input controllers to longitudinal bio-sensors, which highlight the efficacy and potential of our approach.

CCS CONCEPTS

• **Human-centered computing** → **Ubiquitous and mobile computing**; • **Computer systems organization** → **Embedded and cyber-physical systems**; • **Hardware** → **Power and energy**.

KEYWORDS

Intra-body power transfer, IBPT, wireless power, on-body devices, wearables, digital jewelry, eTattoos, sensing, ubiquitous computing

ACM Reference Format:
Andy Kong, Daehwa Kim, and Chris Harrison. 2024. Power-over-Skin: Full-Body Wearables Powered By Intra-Body RF Energy. In *The 37th Annual ACM Symposium on User Interface Software and Technology (UIST '24), October 13–16, 2024, Pittsburgh, PA, USA.* ACM, New York, NY, USA, 13 pages. https://doi.org/10.1145/3654777.3676394

Figure 1: Power-over-Skin allows a single worn transmitter (e.g., stored in a pocket) to provide power to a constellation of small, worn, battery-free devices. Example devices we created include (clockwise from top-left): a controller ring that sends user input over BLE, earrings that blink, a sun exposure monitor with an e-ink display, and body temperature patch that logs data every five minutes.

1 INTRODUCTION

Continued advances in microcontroller design have yielded power-efficient, inexpensive, and yet powerful processors. For instance, the 20 MHz ATTiny85 with 8KB of integrated flash costs around $1 USD [1]. Perhaps the pinnacle of this feat of miniaturization are Apple's AirPods — sophisticated real-time audio processors with wireless streaming connectivity that last hours on a single charge. However, the 0.182 Wh battery in the latest AirPods Pro 2 is by far its largest component [6]. Indeed, batteries pose a significant design obstacle for wearable device creators (e.g., rings, earrings, AR glasses, and similar small devices), both from a physical design (e.g., bigger batteries can preclude desired form factors) and user experience standpoints (e.g., smaller batteries necessitate frequent recharging). Moreover, there are classes of devices we may wish to wear or affix to our bodies (e.g., bio-sensors) that are not as convenient to charge as simply removing an AirPod from our ears.

In response, we investigated an emerging technique of powering on-body computing devices using the human body as the energy delivery medium (Figure 1). We call our technique Power-over-Skin. Prior work has found that the human body is particularly efficient at conducting 40 MHz RF, while largely confining transmitted power to the body [11]. Our system uses a single, worn, battery-powered transmitter to couple RF energy to the user's body (Figure 5). This transmitter can be placed anywhere on the user, and could even be integrated into existing devices such as a smartwatch or the face pad of an AR headset. Since the coupling is capacitive, our technique also works through clothing, and thus can even be integrated into a phone to couple to the user's body through the pocket fabric. When touching the skin, our tiny receiver board (Figure 8) can harness this body-conducted power to support a constellation of distributed, worn, battery-free devices. We receive enough energy across-body to power several applications, including a Bluetooth ring with a joystick, a stick-and-forget medical patch which logs

UIST '24, October 13–16, 2024, Pittsburgh, PA, USA

ACM ISBN 979-8-4007-0628-8/24/10
https://doi.org/10.1145/3654777.3676394

data, and a sun-exposure patch with a screen — demonstrating user input, displays, sensing, and wireless communication. We believe that Power-over-Skin can not only extend the battery life of existing devices and also allow them to shrink further, but enable entirely new categories of small worn computers in locations previously impossible.

Building off prior work, we demonstrate high power delivery at across-body distances, while still maintaining consumer viability by using small (<10 cm^2), dry fabric electrodes for body-coupling. Our technical improvements were enabled by a suite of experiments showing the effects of varying key design parameters (TX waveform, RF circuit design, TX/RX body placement), which, along with our open-sourced electrical design, enable other researchers to use and extend our work. The capabilities enabled by Power-over-Skin allow previously infeasible applications spanning compute, sensing, display, and wireless communications, which are demonstrated in our array of demos. May the following advance the generalisability and illustrate the potential of intra-body power transfer.

2 RELATED SYSTEMS

To situate our research among many efforts in this domain, we now review other systems and technical approaches that relate to Power-over-Skin. Note that after this section, we discuss Principles of Operation, which references non-systems related work.

2.1 Wearable Energy Harvesting

Power sources impose perhaps the strongest limitation on the size and convenience of wearable devices. To decrease form factors further, researchers have investigated alternative power schemes that capture power rather than carrying it. A historical example is the "automatic" or self-winding mechanical wristwatch, which captures arm motion to crank the watch's mainspring. More recently, Teng et al. [26] used mechanical arm exoskeletons to harvest energy from user motion, using the energy to later render haptic effects that enhance the wearer's VR experience. Mechanical approaches can offer significant harvested energy, but they can impede user experience. More compact forms of energy harvesting have relied on other environmental phenomena. Past work has used solar cells for capturing light [8, 12, 17, 19, 20], antennas to capture ambient RF energy from power lines [2, 4, 11], and piezoelectric elements for capturing audio and vibration energy [24, 25]. While convenient and powerful enough for simple sensing and communications, a major drawback of using energy harvesting is its inconsistency. Most devices rely on a steady supply of power, and users' needs require on-demand uptime. When energy sources like light, RF, and sound are blocked by clothing or the body, their usefulness declines.

2.2 Wireless Power Transfer

For more consistent power, researchers have also investigated wireless power. Instead of relying on opportunistic environmental energy capture, receiver devices can depend on stable, constant power emitted from a transmitter in the environment. Many mediums exist for this. Over short ranges, inductive charging can power electronics from static (e.g., Qi charging) and wearable [31] form factors. For farther-field applications, cross-room power transfer

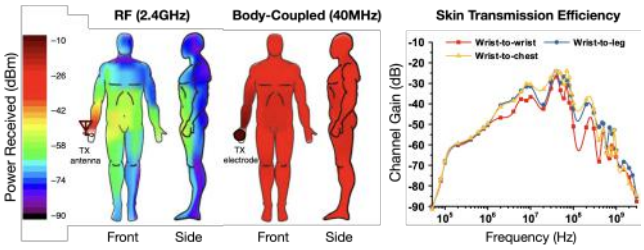

Figure 2: Left: Power transmission pattern on the body from a hand-held transmitter emitting 2.4 GHz and 40 MHz at 0 dBm. Gain measured at body surface. Right: Body transmission vs. frequency for three body-location pairs. Note the peak around 40 MHz. Figures reproduced with permission from Li et al. [11] and included for quick reference.

was previously demonstrated by Iyer et al. [7], utilizing a high-power near-infrared laser on a pan-tilt mount to direct light at a smartphone with a solar panel back. Another approach that avoids the need for precise targeting is RF energy transmission. PowerCast produces 915 MHz transmitters and corresponding receivers which rectify the airborne signal into a regulated DC voltage. This power can then be used to power or charge devices placed in front of the transmitter [18]. True room-scale power transfer has also been demonstrated by Sasatani et al. [21], using magnetic fields to transfer up to 50 W wirelessly. However, these systems generally require specially instrumented rooms.

Though power can be delivered consistently through various forms of electromagnetism, power transfer efficiency is low and requires an environment instrumented with transmitters. The approach becomes less compelling for powering wearables which are expected to leave structured environments with their users. Additionally, a wearable transmitter may not even be possible due to the body-shadowing effect. As demonstrated in the leftmost plot of Figure 2, the body itself blocks high-frequency RF signals, such that a worn antenna may not be able to reach around the body to deliver power to wearables everywhere [11]. A more efficient approach would confine the transmitter power signal to the skin, where worn devices can expect capacitive coupling or direct contact.

2.3 Intra-Body Power Transfer

Past researchers have used the body to power devices through touch. This method, called intra-body power transfer (IBPT), shares many underlying principles with body area networks [14, 27], but with the added requirement of maximizing power throughput. Because power is confined to the skin surface, IBPT achieves total body coverage in contrast with wireless RF power transmission, and requires no targeting to reach receiver devices.

An early example is TouchTags [28], which used an RF transmitter embedded in the shoe to enable a wearer to power up and read an RFID tag through touch. Their system required the receiver RFID tag to be coupled closely to earth ground, and could not be implemented into wearable, mobile devices. More recently, CASPER [29] placed RF transmitters into objects (beds, chairs, jacket) that a user would "serendipitously" contact for long periods to charge their wearable devices. Their final implementation used a 13.56 MHz RF

transmitter to charge up a decorative arm patch with LEDs at an average rate of 248 μW. The power rate of their implementation is enabled primarily by their ground electrode size (>50 cm^2), which limits the application design space.

Showcasing more complex interactions, SkinnyPower [23] used a closely-spaced transmitter and receiver placed on the wrist and finger respectively, achieving a received power of 1003.8 μW using a 100 MHz carrier wave. Their transmitter was able to power a microcontroller, read an IMU, and emit Bluetooth packets at ~1 Hz. Using an RF amplifier, their ground electrode could be reduced below 10 cm^2, enabling smaller form-factors like a ring, but only across limited on-body distances (<15 cm). The same authors extended this work in ShaZam [13], adding impedance matching with environmentally-anchored transmitters.

Though sufficient power had been shown, the limited on-body ranges still restricted wearable applications using IBPT. Li et al. [11] achieved long transmission distances using an LC resonance circuit on the receiver. A transmitter worn at the wrist could power calculators at the other hand, ankle, and neck, transferring 2 μW from head to toe. Despite reaching everywhere, their received power is insufficient for powering wearable devices, which require upwards of 100s of μW. Additionally, their use of disposable gel electrodes hampers consumer applicability.

Prior investigations into IBPT have shown promise for enabling battery-free receiver devices distributed across the body powered from a single battery-powered transmitter. However, implementations thus far have only transmitted sufficient power across limited ranges (<15 cm), across body at limited power (<10μW), or using large electrode sizes (>50 cm^2), holding back adoption by consumer devices. We designed Power-over-Skin with these limitations in mind, optimizing power transfer across-body and enabling previously infeasible worn locations.

The advances made in this work allow receiver devices with ground electrodes substantially smaller than those used in CASPER (see Figure 5), delivering similar power as SkinnyPower, with the full-body coverage of Li et al. [11], all while using dry fabric electrodes. These advancements collectively address key challenges in IBPT, potentially accelerating its adoption in consumer devices. Our work builds upon valuable experiments done in prior research and represents a significant step forward in making IBPT more practical and widely applicable.

3 PRINCIPLES OF OPERATION

We now provide a brief primer on the main principles of operation behind Power-over-Skin, and IBPT more broadly.

3.1 Human Body as a Transmission Medium

When using the skin as a conductive medium, it helps to understand the electrical characteristics to best optimize our implementation. The human body can be modelled as a complex RC circuit. Since we wish to have only one connection point to the body on the transmit and receive side, we must rely on the body's capacitance and use high-frequency AC waves (RF) to conduct energy. Though the precise values of the human body circuit vary from person to person, this variation is negligible at the higher frequencies we need to use [15]. From this understanding of IBPT as energy transfer across the human capacitance, we can begin to make choices regarding our system.

First, IBPT efficiency can be improved by adding impedance-matching networks at the skin-electrode junction, but only at a predetermined frequency. Thus, choosing the frequency of the power carrier wave is one of the first steps in designing such a system. Past investigations show that human skin transmittance exhibits a complex frequency response, as shown in Figure 2. Frequencies with the highest channel gain will maximize power delivery — these peaks occur around 40 MHz and 100 MHz. Since lower frequencies are (generally) simpler to generate and offer less radiative losses from the body than higher frequencies, we chose to use 40 MHz as our primary power transmission frequency.

After choosing a carrier frequency, we can begin to optimize the RF power path through the body. The main losses stem from reflections at skin-circuit interfaces and resistive losses within the transmission medium. In RF systems, these properties are described by coefficients known as S-parameters, with S11 describing reflections and S21 describing channel gain. Since our channel, the skin, cannot be modified, we focus instead on minimizing reflections, i.e. S11. When an RF signal passes between two mediums with different impedances, the mismatch will reflect some signal power. This significantly reduces efficiency since much of the transmitter energy does not make it into the skin. An impedance-matching network made of passive components (inductors and capacitors) can be used to match the transmitter's output impedance to the medium's impedance, mitigating reflection.

3.2 Safety

Systems where electricity makes contact with the human body must keep safety a core consideration. We refer to the 2020 International Commission on Non-Ionizing Radiation Protection (ICNIRP) guidelines on limiting exposure to time-varying electromagnetic fields [5].

Lower frequency signals (<100 kHz) can induce perceptible effects on nerve and muscle tissue (i.e., parasthesia, muscle activation) as they oscillate, as well as causing generalized tissue heating. However, since human nervous tissue does not react quickly enough at frequencies higher than 100 kHz, the guidelines from 100 kHz-6 GHz are primarily concerned with preventing heating-induced localized tissue damage through excessive energy concentration. These high-energy "hotspots" can occur when the RF power is low but passing through a small contact area, or when total RF energy is excessively high. These are quantified and referred to as the specific energy absorption rate (SAR, units of W/kg), contact current intensity (units of mA), and the total induced current (units of mA). Throughout the development of our system, we carefully designed our transmitter stage with these metrics in mind.

The ICNIRP 2020 guidelines specify limitations for contact current only for high-powered emitters like radio stations, a threshold our transmitter is not capable of reaching. Additionally, we found during testing that even single-point skin contact with our transmitter wave produced no perceptible sensation of heating or pain in any participant. Nevertheless, in the interest of safety, our transmitter contact electrode is sized as large as possible to avoid this. Beyond single point current, ICNIRP also specifies a maximum total body

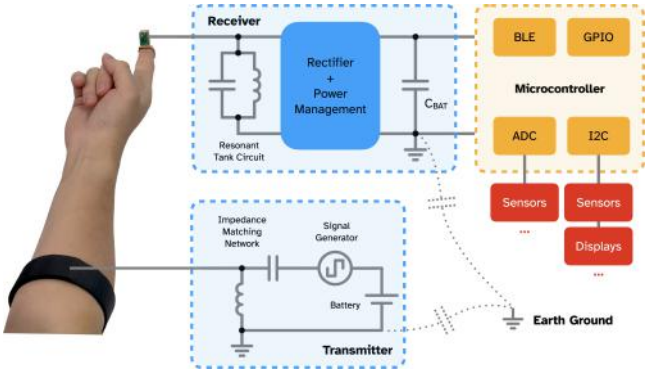

Figure 3: Overview diagram of our implementation of Power-over-Skin and the path that power takes. Dotted lines represent parasitic capacitors to earth ground.

current of 45 mA. With the inclusion of the impedance-matching circuit, the output current of the Power-over-Skin transmitter cannot exceed 17 mA. This figure is further reduced when including the transmitter output impedance and the skin impedance.

With current safety satisfied, we move on to SAR. This describes the rate at which RF energy is absorbed by body tissue in W/kg. Limits are specified in order to avoid elevating core body temperature beyond 1°C, which can increase cardiovascular load and cause a higher rate of accidents. ICNIRP restricts whole-body average SAR to 80 mW/kg for the general public in the frequency range 100 kHz-6 GHz, targeting a maximally tolerable 0.1°C increase in body temperature [5]. Computing maximum whole-body SAR using the average body weight of an adult human female (62 kg from [3]), we arrive at a figure of 4.96 W. None of our transmitters could output that much power.

4 IMPLEMENTATION & EXPERIMENTS

Development of a complex system such as Power-over-Skin requires selecting and balancing priorities. Throughout development, our chief performance metric was maximizing receiver power in order to drive rich end uses, such as on-body sensing. Our highly-iterative development process relied on scores of small empirical experiments to quantify effects and make technical progress. In this section, we endeavour to provide an overview of our research process and how different experimental findings informed our design. We organize our discussion according to the flow of power, starting with the transmitter, through the circuit-skin interface, the Power-over-Skin receiver, and finally end-user applications. Figure 3 provides a overview of Power-over-Skin.

4.1 Measuring Power

Before we discuss our implementation, we wish to clarify our measurement procedure.

Wireless power systems (such as our own) are difficult to test, because taking measurements can change the performance. For example, the receiver power of Power-over-Skin is primarily bottlenecked by the low capacitive coupling between our receiver ground and environment (<1 pF estimated). Naively probing the receiver substantially improves the ground coupling, and unrealistically increases the measured performance.

Our closest related work, SkinnyPower [23], used oscilloscope probes to measure received power, adding 16 pF of capacitive loading to their receiver ground circuit. To mitigate these loading effects, Li et al. [11] used an analog buffer with 1TΩ of input impedance in front of a battery-powered oscilloscope probe, adding only 2.1 pF. However, even this requires running a long, ground-shielded oscilloscope cable to the device.

4.1.1 Measurement Apparatus. To minimize additional ground coupling, we need a buffered measurement device which adds as little ground coupling as possible. To do this, we built a small, battery-powered multimeter using an ESP32 microcontroller. Unnecessary ground coupling is avoided by keeping the circuit battery-powered and as compact as possible. The storage capacitor voltage of a Power-over-Skin receiver board is buffered through an op-amp with high input impedance (10TΩ, SM73307) and digitized by the ESP32, which streams the data to a laptop via BLE. This measurement is more isolated than measurements in prior work as the ESP32 shares no physical connection with earth ground. This untethered system can also be worn in the same body locations that end-user apps might use, allowing us to collect data in scenarios that reflect real world use.

4.1.2 Measurement Method Impact on Power. To quantify the accuracy of different measurement methods, we ran a head-to-head evaluation. Without moving, a participant wore a transmitter and Power-over-Skin receiver on their arm, located 10 cm away from each other. An experimenter attached one of three measurement devices to the receiver: 1) oscilloscope probe (DS1054Z stock probes, 10x attenuation), 2) our own wireless multimeter, or 3) a 10 cm^2 copper tape ground plane. Since we do not directly measure the receiver voltage in the latter setup (3), we instead recorded the LED blink rate of our receiver board with a high-speed camera to calculate received power.

Results showed significant differences among the measurement methods. In the oscilloscope condition, the storage capacitor sat at 3.75 V while the LED stayed persistently on. Assuming a 1.7 V LED forward drop and a 1kΩ resistor, the oscilloscope-connected receiver board continuously received ~7.24 mW of power. With our wireless multimeter, we recorded power transfer of 294 µW (and observed an LED blink rate of 1.39 Hz). Finally, our bare board with copper tape ground plane blinked at 0.37 Hz, which we estimate to be roughly 78.3 µW (assuming energy proportional to multimeter blink rate).

Note that the oscilloscope measurement gives nearly a 100× overestimate compared to lone-receiver power. Our wireless multimeter is more accurate, through still ~3.75× what we consider to be the true received power. We believe the bare board measurement is the most realistic estimate of intra-body power transfer, as it occurs under conditions closest to real-world. Nonetheless, we employ our wireless multimeter in nearly all subsequent experiments, as capturing fine-grained harvesting data was critical for development and power management. However, the relative scalars in power between these measurement conditions are important to keep in mind, especially when comparing to other systems.

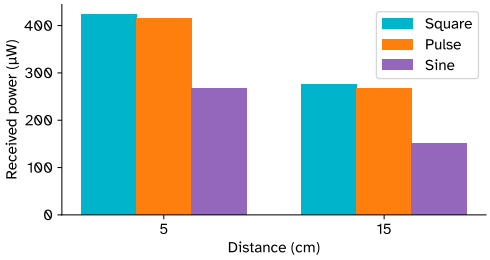

Figure 4: Received power vs. power carrier waveforms at 40 MHz, 10 Vpp. Receiver worn at the wrist, with the transmitter placed 5 cm and 15 cm away on the arm.

Figure 5: In addition to a basic velcro strap (seen in Figure 14), we created three prototype transmitters built into existing objects: phone, XR headset, and shoes.

4.2 Power Transmission

We now describe the first half of our system: power transmission.

4.2.1 Waveform Selection. IBPT systems in the past have exclusively used sine waves as their power carrier. However, during testing, we discovered that square waves transfer more power at the same peak-to-peak voltages. As a bonus, they are also easy to digitally generate, and for all our experiments we use a square wave transmitter. We believe the increase in received power is due to the higher-order harmonics also contributing to power delivery (notably 120 MHz, the 3rd harmonic of 40 MHz, which is also an effective frequency for IBPT; see Figure 2). We verified our hypothesis with an experiment, the results of which are seen in Figure 4. For a fixed transmitter/receiver setup, a square wave transmitter exhibits a ~75% increase in received power compared to sine waves.

4.2.2 Proof-of-Concept Transmitter. We invested most of our efforts in optimizing our worn receivers, where size, weight, form factor and power efficiency are paramount. As such, we often used a bench-top signal generator (Siglent SDG5162) to synthesize our RF signal on the transmit side. Although this offers a better connection to earth ground compared to a battery-powered transmitter, it still approximates the performance of worn transmitters in our applications because the receiver ground plane is the more significant limitation on our power transmission. This was used for all experiments in this implementation section.

For our example applications, we did create several worn transmitter prototypes, which can be seen in Figure 5. For these, we used an ESP32 to output a 40 MHz square wave (an integer divisor of its 160 MHz base clock frequency) at 3.3 Vpp. This signal was then fed into an RF amplifier board (p.n. TQP3M9009) with a nominal gain of 27.36 dB, the output of which is impedance matched before connecting to the body-coupled electrode.

4.2.3 Transmitter Impedance Matching Circuit. While human skin impedance reaches a minimum around 40 MHz (see Figure 2), many factors interact to affect power. As noted earlier, one important consideration is impedances-matching at the electrode-skin interface. We added an LC circuit to the output of our transmitter to match the RF amplifier's 50Ω output impedance with the skin's impedance at our power carrier frequency. Skin impedance measurements were taken from Muramatsu and Sasaki [15].

In an LC IMN, either the inductor or capacitor is placed in series, with the other component shunted to ground. For single-frequency transmission, which component shunts to ground does not matter because the output impedance will still be matched. However, our implementation of Power-over-Skin uses square waves, which are made of the sum of the sine waves at the fundamental frequency and all the higher odd harmonics. Since these higher frequency harmonics also contribute to power delivery, we must design our LC circuit with attention to detail. In simulation (PathWave ADS) and in testing, we found that using an inductor to ground offers a lower S11 for higher frequencies, thereby delivering more power into the skin compared to capacitor to ground. We use this configuration in our transmitter design.

4.2.4 Circuit Design. Since capacitive power transfer varies significantly with frequency, care must be taken in component selection or PCB design. For example, all inductors self-resonate with their parasitic capacitances at a specific frequency, and past this point they no longer function properly as inductors. For common inductors, this happens well below 40 MHz. Accordingly, we chose high-quality RF inductors intended for these higher frequencies. Additionally, large package sizes can add parasitic effects, degrading performance or shifting the IMN peak frequency. We chose the smallest usable components for our boards to minimize these effects. Though our carrier frequency sits below "leakier" higher RF perspective, we still need to avoid some common low-speed design patterns lest they impact power efficiency. For example, unused PCB area is commonly filled with a copper ground plane for decoupling. But in our receiver, this adds stray capacitance to the RF path, radiating away received power or shifting the resonant peak frequency. Finally, long, thin traces should be avoided, since they can add unintended inductance.

4.2.5 Transmitter Ground Size. We investigated if ground electrode surface area effects transmitted power. For this, we placed a transmitter at the wrist and a receiver board on the finger tip, 20 cm away. We fixed the transmitter electrode size and material, and compared power transmission performance for different transmitter ground electrode surface areas (from 0 to 50 cm^2 in 5 cm intervals). Our results (Figure 7) show that transmitter ground area does not affect delivered power. We believe this is because the transmitter is well grounded and is not the limiting factor for power transmission in our circuit.

4.2.6 Transmitter Electrode Size. Using a similar experimental setup, we then investigated transmitter body-coupled electrode size. In this experiment (results seen in Figure 7), we varied the body-coupled

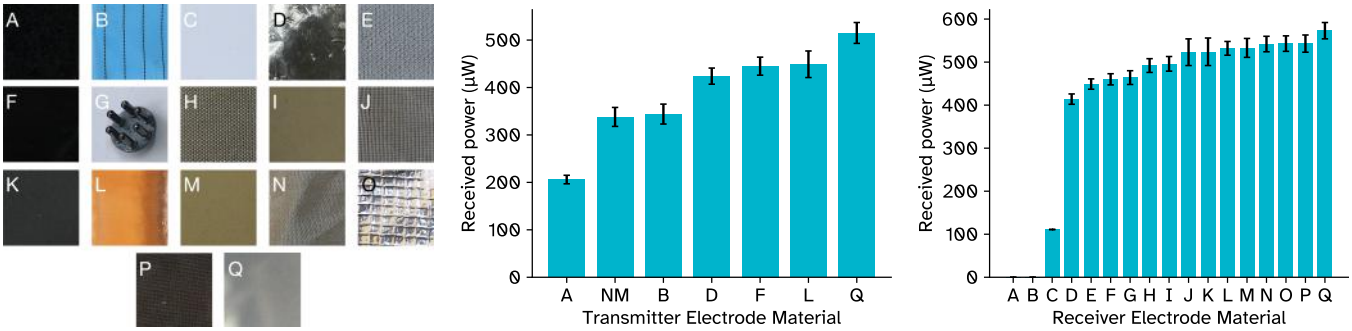

(a) Materials (b) TX Power (c) RX Power

Figure 6: Materials (a), close-up texture of each material tested as transmitter and receiver electrodes. A - conductive foam, B - anti-ESD fabric, C - 20 lbs. printer paper, D - aluminum duct tape, E - Knit Jersey Conductive Fabric (Adafruit 1364), F - conductive rubber (Western Rubber & Supply RX 230-2250), G - Ag/AgCl-coated electrode, H - shielding tape (3M CN-3190 EMI), I - Nolato 8650, J - ArgenMesh, K - Nolato 8641 conductive silicon, L - copper tape, M - Nolato 8633, N - Woven Conductive Fabric (Adafruit 1168), O - AL60 Wall Shield (LessEMF 12273-FT), P - Stretch Conductive Fabric (LessEMF 11321-FT), Q - ITO-coated plastic. TX Power (b), performance of different transmitter electrode materials on received power. RX Power (c), performance of different receiver electrode materials on received power.

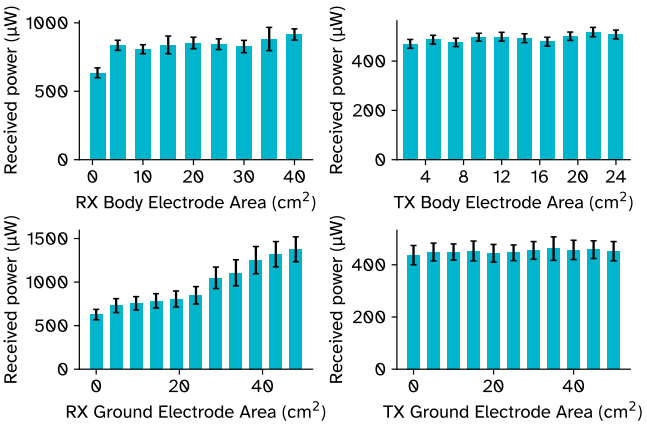

Figure 7: Received power as a function of receiver ground and electrode surface area, and as a function of transmitter ground and surface area.

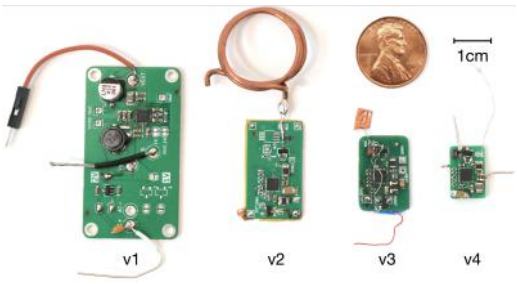

Figure 8: Major milestones in the iterative development of our receiver board. We used our v4 board to create all of our example applications. Penny included for size reference.

electrode surface area from 2.4 to 24.0 cm^2, in 2.4 cm^2 intervals, and measured the received power. Like our previous result, we found little change in received power with respect to electrode size.

4.2.7 Transmitter Electrode Material. Next, we sought to optimize our transmitter electrode material. While wet electrodes offer low impedance coupling to the human body, they can dry out, irritate the skin, and require frequent replacement. For these practical reasons, we did not consider them. Instead, we tested seven dry materials (A, B, D, F, L, and Q in Figure 6a). For this experiment, we held constant TX-RX position (wrist-to-fingertip), ground electrode size (12.5 cm^2), and body-coupled electrode size (12.5 cm^2). The receiver board used a 2.5 cm^2 copper patch for its body-coupled electrode.

Our experiment results (shown in Figure 6b) reveal there are significant performance differences across materials. All conductive materials exhibited similar power transmission, while less conductive materials like the conductive foam (material A) and anti-ESD fabric (material B) impeded transmission. We were surprised by the efficacy of these high-impedance materials, and so we also included a "no material" (NM) condition by disconnecting any conductive elements between the transmitter and the skin. We found that no material (NM) performs comparably to the insulating anti-ESD fabric, possibly since both couple in power capacitively. The best performing material was an ITO-coated plastic sheet (material Q in Figure 6a). However, since ITO suffers from oxidation, we instead chose a silver-coated nylon fabric (material P [10]) as our transmitter body-coupled electrode material.

4.3 Power Reception

We now describe the development considerations of our receiver board, which went through many iterations to reduce size and increase received power (major milestones shown in Figure 8).

4.3.1 Board Design. As with the transmitter, careful board design of the receiver is paramount to high performance. We avoided PCB ground fill near the RF input, reducing stray capacitance that would reduce input RF. Additionally, the RF input was kept physically short to minimize any parasitics, and the components used are among the smallest sizes for their rated values and voltages.

4.3.2 Receiver Resonant Tank Circuit. A large obstacle in the implementation of any IBPT system is the minimum voltage required to receive power. First, any incident RF on the receiver board below ~200 mV in amplitude does not make it past the rectifier diodes since it is lower than their forward voltage. Then, after the rectifier diodes produce a DC voltage, our board uses a micro-power management IC to store energy into a capacitor. The cold-start voltage of this chip is 600 mV, below which no power is stored. Because the voltage requirements are the primary bottleneck for collecting energy, we shunt the input to ground with a resonant tank circuit (similar to Li et al. [11]) in order to increase the input voltage on the receiver side. By choosing LC values that maximize RX_in impedance at the power transmission frequency, our circuit resonates with the incoming RF wave at the transmission frequency, boosting the input voltage and allowing the receiver to store power even in conditions where the peak-to-peak voltage is too low for an ordinary input stage.

4.3.3 Receiver Electrode & Ground Design. For ease of integration into tiny wearable devices, we wanted to keep the Power-over-Skin receiver board as small as possible — however, using a small board also limits skin contact area and the capacitive return path formed with earth ground, directly limiting received power. Any body-coupled electrode or ground electrode area must be added post-hoc depending on application requirements. In order to precisely balance these two forces while maintaining a small footprint, we ran a series of experiments to quantify the effects of different body-coupled electrode materials and surface areas, as well as ground plane areas, on the received power.

4.3.4 Receiver Electrode Material. As an experiment, we had participants wear a transmitter strap at the wrist and place their hand on a table such that their middle finger rested near, but not touching, a receiver's power input lead (on-body distance 20 cm). Various electrode materials cut into 2.5 cm squares were laid over the receiver's input lead, bridging the gap between the participant's finger and the receiver (see Figure 6a). Received power was recorded for a minute or until the power stabilized (results in Figure 6c).

Thicker materials like the foam (material A) performed poorly despite being electrically conductive, likely because increased thickness decreases the capacitive coupling between the skin and electrode. The anti-ESD fabric (material B) totally blocked power delivery — when measured with a multimeter, we discovered that the fabric was insulating and only the thin black threads were conductive. Paper (material C) was used as a control to measure power transfer without an electrical conductor. In this configuration the participant placed their finger slightly forward to allow for capacitive coupling with the electrode. Finally, all of the conductive fabrics performed similarly to the metal tapes (copper and aluminum), with the best-performing material being an indium-tin oxide (ITO) coated plastic (material Q). Like our transmitter, we chose a more comfortable and durable silver-coated nylon fabric (material P) for our receiver electrode.

4.3.5 Receiver Electrode Size. For devices worn at the extremities, the receiver's body-coupled electrode size is a limiting factor. We investigated the effects of the receiver electrode's contact area on received power. A participant wore a transmitter at the wrist, with their hand placed palm-down over a large patch of copper as the receiver body-coupled electrode. After each measurement, the experimenter removed 1 cm of the copper electrode until only the lead wire remained. Results are shown in Figure 7. Received power decreases slightly with contact electrode area, but only becomes significant as the size falls below 5 cm^2. We believe this is because the increased contact area does not significantly improve the skin-electrode impedance once reliable contact has been made.

4.3.6 Receiver Ground Size. Due to our receiver board's tiny size, on-board ground coupling is minimal, and any added ground plane significantly boosts received power. This posits a delicate balance, since additional grounding also increases the receiver size, limiting potential on-body locations. To quantify the effects on power, we ran an experiment varying receiver ground plane area using the same setup as the previous experiment. Instead of placing the palm on the receiver electrode, the tip of middle finger touches it instead (20 cm on-body distance). The receiver ground is attached to a long strip of copper tape (20 cm long × 2.4 cm wide) extending away from the receiver board. After recording each power measurement, the experimenter would cut 2 cm off of copper tape until no more remained (i.e., incrementally shortening the receiver ground size). Results can be seen in Figure 7. Compared to the other surface area experiments, varying receiver ground surface area has the largest effect on received power, confirming our hypothesis that environment to receiver ground coupling is the limiting factor in power transmission for our current implementation.

4.3.7 Energy Storage. Our receiver board uses capacitors for storing energy, primarily for their compact size and robustness. Because of limited power transfer, the storage capacitor should be carefully sized for each application — for instance, our LED earring demo (Figure 12) benefits from frequent blinking and can use a smaller capacitor, while our medical patch application (Figure 14) needs to stay awake long enough for the microcontroller to boot, read sensor data, and transmit a Bluetooth packet, necessitating a larger capacitor. Capacitor choice is further constrained by material composition. Ceramic capacitors are widely available, but can lose capacitance as their rated voltage is reached. Other capacitor materials like tantalum or aluminum are more stable, but are larger and have higher leakage currents. We use tantalum capacitors for all of our receiver boards.

4.4 Powering Microcontrollers

Once our receiver board has accumulated energy in its on-board capacitor, it can use that power for anything — in our simplest design, an is LED blinked whenever the capacitor fills up, and we used this extensively for debugging and power estimation. However, a more compelling use for power is for running a microcontroller, which can drive displays, read sensors, and communicate wirelessly.

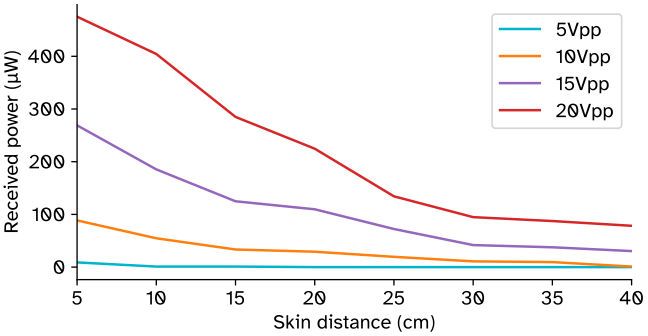

Figure 9: Received power at the wrist from a transmitter placed at varying distances along the arm. The transmitter outputs a 40 MHz square wave at various amplitudes, and uses our impedance matching circuit to couple to the body.

As a proof-of-concept, we used our receiver board to power a Seeed Studio XIAO nRF52840 [22] (64 MHz ARM Cortex-M4), using a 200 uF tantalum capacitor for storage. At full charge, this only powers the microcontroller for a few hundred milliseconds. However, this still enough to enable interactive applications. The microcontroller can be configured to wake up in response to interrupts from external sensors or buttons, or alternatively, to wake up at preset intervals to perform a burst of processing (e.g., wake every second, read a sensor, sleep again). Between wake-ups, the microcontroller stays in light sleep (~25 µA) if we need to store variables in volatile memory or deep sleep (~5 µA) if not. The nRF52840 is BLE-capable and can communicate wirelessly with other devices (e.g., phones and laptops). In practice, our energy budget allows data transmission only once every ~500 ms, though we note that this is sufficient to support many interactions (see e.g., our subsequent ring demo in Figure 13).

5 OPEN SOURCE HARDWARE

To enable other researchers to replicate and extend our work, we have made our circuit designs available at:
https://github.com/kongmunist/Power-Over-Skin-Hardware

6 SYSTEM EVALUATION

In Section 3, we were able to draw on the experiments from prior work to establish the basic operating principles of our system. Then in Section 4, we discussed many foundational experiments that informed the iterative development of our implementation. In this section, we evaluate the performance of our final prototypes on-body in a realistic experiment.

6.1 On-Body Location & Transmission Distance

Power-over-Skin provides a high degree of freedom when choosing where to place transmitters and receivers across the body. Crude estimates for available power at various TX-RX pairings are possible using the data visualized in Figures 2 and 9, but power transfer depends on many factors. To better determine realistic power budgets, we ran a point-to-point power delivery experiment with three participants. Specifically, we investigated four transmitter locations: sole of the right foot, abdomen (to the immediate left of the belly button), left wrist, and face (specifically the infraorbital region below the eyes, where an AR/VR headset would rest). Each of these was fully crossed with six receiver locations: right ankle, back of the neck, sternum, left bicep, right bicep, and left index finger metacarpal. Each site was chosen to match common wearable placements. Measurements were recorded at each receiver position in a random order for each transmitter placement. This yielded 24 paired measurements per participant.

The receiver board used silver coated nylon fabric (22 cm^2, material P) as its body-coupled electrode and copper tape as the ground electrode (15 cm^2), and was secured to the body with straps. Received power was measured using the previously-described wireless multimeter offset from the body using a small square of foam to prevent body-ground coupling attenuation of the receiver power path. For each body location paired measurement, we recorded one minute of data or until the power measurement stabilized, using the charging rate of a storage capacitor (100 uF) to calculate the received power in watts. A bench-top function generator outputting a 40 MHz square wave at 10 Vpp was used as the power wave source. This signal was sent through the impedance matching network, then coupled to the body using the same silver coated nylon fabric (20 cm^2) as the receiver. Participants stood on a carpeted floor in a neutral pose, with arms by their sides. The results of this experiment are seen in Figure 10.

6.1.1 Discussion. As anticipated, there is only an approximate relationship between on-body distance and received power. Another significant effect to note is the decrease in power at more central receivers, probably resulting from the large body plane at those locations coupling to the receiver ground. At more distal sites like the fingers or biceps, received power increases since the body does not couple as tightly to the receiver ground. Nevertheless, body distance is still significant. The highest recorded power (1.53 mW average) occurred at the shortest distance, when transmitting power from the left wrist to the left index finger. Correspondingly, the lowest power (5.3 µW average) was recorded at one of the furthest TX-RX body distances, from left wrist to right ankle.

As power is available anywhere, devices can be placed across the body with relative impunity as long as a lower duty cycle is acceptable. Most TX-RX locations cannot support continuous microcontroller operation, and any applications must choose their TX-RX locations carefully depending on requisite uptime. As an example, a biomedical patch which needs to wake-up to record data every hour must be placed in a site where it can save up enough received power over the hour to sustain its operation. Additionally, if a microcontroller is used, the received power must be high enough to sustain its sleep state, or else it will be required to persist data into nonvolatile memory to survive an unexpected shutdown.

6.2 Through-Clothing Transmission

As noted in previous IBPT systems (and quantified in CASPER [29]), power transmission is possible even across small skin-electrode gaps, albeit with reduced efficiency. As a supplemental experiment, we measured point-to-point power using a transmitter placed in the pocket, coupling to the same three participant's bodies through

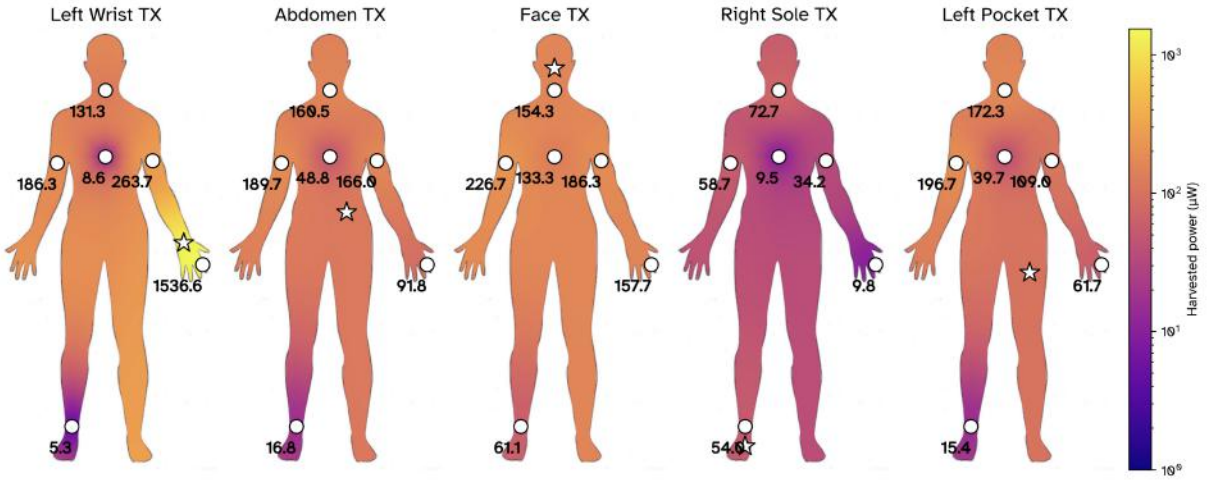

Figure 10: Received power for 24 pairs of transmitter-receiver locations across the body. Circles indicate receiver placements, and stars denote transmitter locations. For the Left Pocket TX condition, the transmitter capacitively coupled to participants' skin through one layer of pocket fabric and one layer of underwear.

their clothes (in all three cases, transmitter and leg was separated by one layer of pocket fabric and one layer of underwear). We tested the same six receiver locations from the previous section. These results can be seen in Figure 10, Left Pocket TX. Overall, we observe that the pocket transmitter delivers similar power as the face-worn transmitter.

6.3 One Transmitter with Multiple Receivers

With just one transmitter, Power-over-Skin can power several receivers simultaneously. As a simple test, a participant wearing a wrist strap transmitter placed their hand face-down on a table, where an experimenter then placed between one and five receiver boards under each finger (starting with the middle finger). Each TX-RX distance was approximately 20 cm. Our Bluetooth power meter was always attached to the receiver held under the middle finger, and measured power was recorded each time a receiver was added. These results are plotted in Figure 11. We can see a small reduction (~20 μW) in the receiver power with each added receiver. However, the reduction is not zero-sum, since each additional receiver consumes approximately the same amount of power as our Bluetooth power meter receiver. This demonstrates that as the number of devices goes up, the total power efficiency also increases.

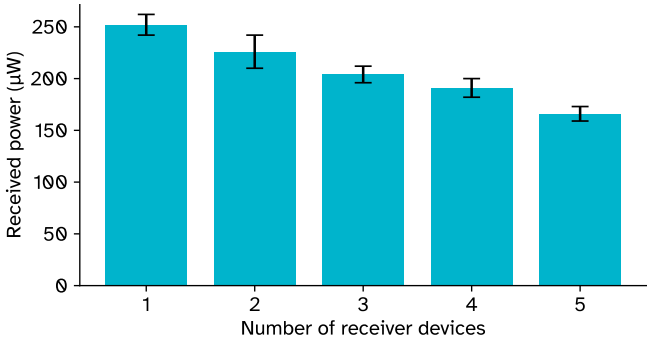

Figure 11: Power received at the fingertips from a wrist transmitter as additional receivers are added (one under each finger). Available power decreases with more devices, but not in a zero-sum fashion.

7 EXAMPLE APPLICATIONS

Prior work has motivated, described, and built innumerable on-body widgets and devices. For this reason, we did not not place significant emphasis on application development. We believe Power-over-Skin has the potential to increase the practicality and lifespan of many of these prior systems, as well as allowing for novel body placements. Nonetheless, we did create several example devices to convey the efficacy of our technical approach, which we describe in this section. As discussed previously, our transmitter can be comparatively large, as it contains the only battery in our system; the power-receiving devices can then be small and lightweight (e.g., our medical patch weighs just 5.4 g). Please also refer to our Video Figure.

7.1 Jewelry

Starting simple, we created an earring with a decorative ground and an LED (Figure 12). Blink rate is controlled by our power management IC, which discharges the storage capacitor across an LED when enough power is stored. The transmitter is contained in a hairband, which can accommodate the weight of batteries better than a small earring.

7.2 Input Ring

Inspired by Zucco and Thomas' design guidelines for wearable pointing devices [32], we created a thumb-worn joystick powered by a wrist-worn (e.g., smartwatch) transmitter. Our ring-like device (Figure 13) is built around an nRF52840 powered by our receiver

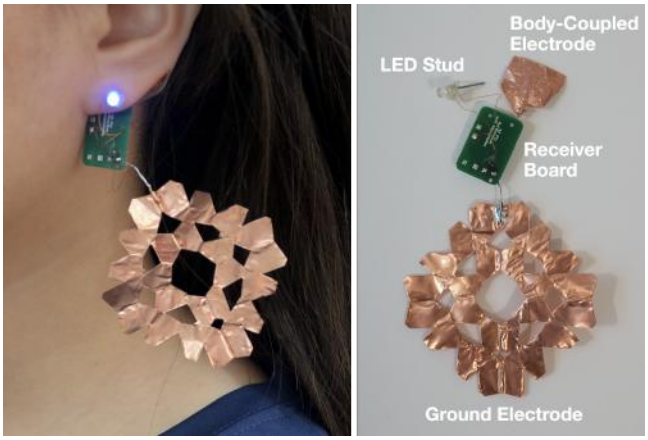

Figure 12: An earring that blinks as an example of Power-over-Skin integrated into jewelry.

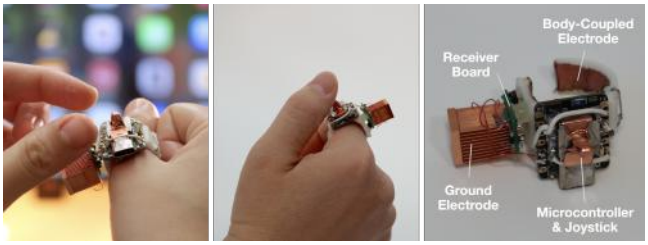

Figure 13: A Power-over-Skin controller ring, allowing users to wirelessly control an interface with a miniature joystick.

board (see Section 4.4). We programmed the microcontroller to read the joystick state (up/down/left/right/click) on wake-up, transmitting it as a BLE beacon packet which can be consumed by any number of listening devices. As a simple demo, we use it to control a TV (see Video Figure), but it also has obvious utility in AR/VR experiences as a fine-grained and convenient input mechanism.

7.3 Medical Patches

Power-over-Skin is particularly suitable for longitudinal health sensing, since changes in bio-signals happen over minutes to hours (as opposed to real-time responsivity, e.g. our ring joystick). Our receiver can store plenty of energy, allowing us to power a microcontroller for an extended sensing operation (e.g., ECG heart rate) and perform a wireless transmission to another device which persists the data. This also means our transmitter can sit further away — for example, in a shoe or phone, as shown in Figure 5. As a simple example, we built a patch which senses body temperature and transmits the measurement over BLE to a laptop.

7.4 On-Body Displays

Many prior on-body displays have been powered using batteries or even wall power (see e.g., AugmentedForearm [16], Klamka and Dachselt [9], SkinMarks [30]). Using Power-over-Skin, we can create entirely self-contained, on-skin displays. Given our tight power budget, we used an E-Ink display, which is visually persistent

Figure 14: Patches for longitudinal biometric monitoring could benefit from Power-over-Skin. As a proof of concept, we built a body temperature monitor that logs readings roughly every five minutes over Bluetooth.

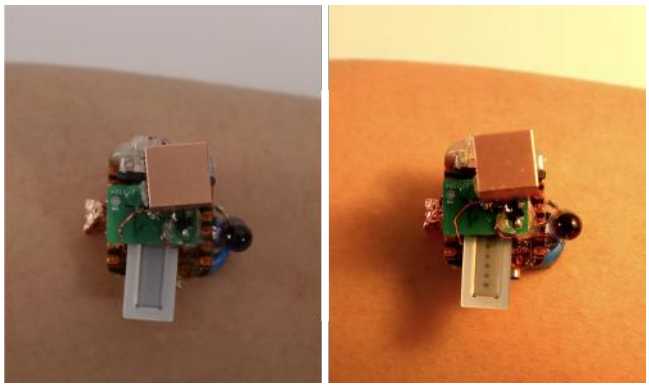

Figure 15: Power-over-Skin can enable on-body displays, such as this sun exposure meter with a five-segment e-ink display.

and expends power only when updated. As a simple demo (seen in Figure 15), we created a real-time sun (UV) exposure monitor which measures light exposure with a photodiode, and displays its intensity on a five-segment E-Ink display (p.n. 1272-1002-ND).

7.5 Calculator

As a final demo, we instrumented an off-the-shelf calculator, covering the solar cell and removing the internal battery (Figure 16, left). To make it compatible with Power-over-Skin, we added our receiver board, a body-coupled electrode, and a ground electrode (Figure 16, right). Unlike our other demos, this is a commercially-engineered product that has been power-optimized, and even with our modest power budget, demonstrates real-time input, output, and computation.

7.6 Envisioned Example Applications

Many applications were considered during development, but are left for future work. For example, we believe digital contact lenses or smart glasses could be powered via Power-over-Skin from a head or neck-worn transmitter. Haptic gloves or a thimble could also be powered remotely, ideally from an XR headset already containing a battery. We note that shoes are a well-suited place to integrate a battery and transmitter. Finally, wireless headphones could tap into IBPT to significantly extend their runtime.

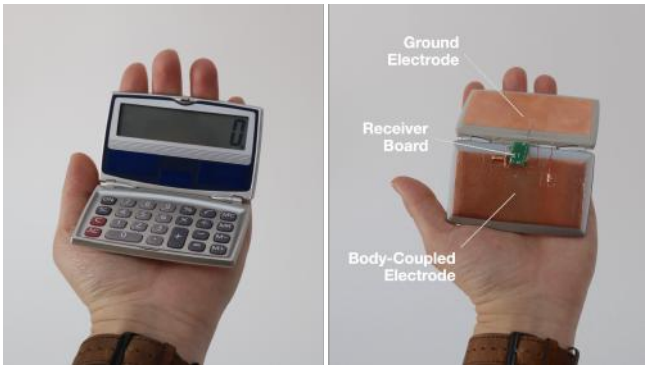

Figure 16: We instrumented this off-the-shelf pocket calculator with a Power-over-Skin receiver board as a basic demonstration of input, output, and computation in one device.

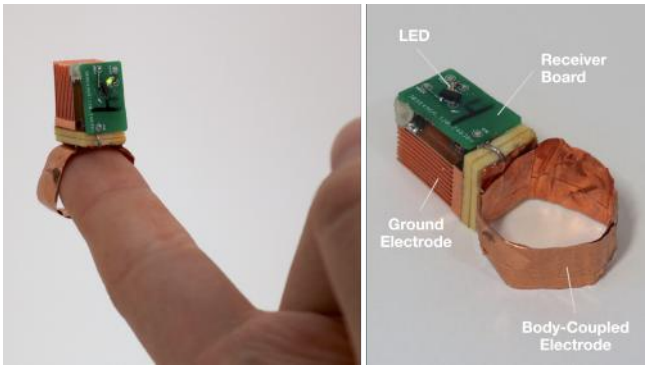

Figure 17: Simple LED blinking circuit used during testing to determine minimum viable size for a receiver. A copper heatsink is used as the ground electrode.

8 LIMITATIONS & FUTURE WORK

8.1 Micropower Limitations

While our applications show that Power-over-Skin supports similar sensing, input, and output features as battery-powered wearables, we note that these features can only be powered intermittently. Even in our highest power configuration (wrist-to-finger), our wireless microcontroller must be duty cycled. For devices that require constant uptime, we imagine that clever integrations of transmitter and receiver into the environment (like those in CASPER [29] and ShaZam[13]) could be made, supporting opportunistic, longer-term charging of a worn device as the user is resting. This long charging period then enables constant uptime when the device is needed. To the user, the need for charging effectively vanishes.

8.2 Environmental Interference

While our transmission frequency is already well-confined to the skin compared to other forms of RF power delivery, some capacitive coupling to other conductive bodies is inevitable. During testing, we observed that capacitive coupling via contact with nearby human bodies can lead to a loss in received power. This is particularly noticeable when the transmission path is long (e.g., from headset transmitter to the hand) and contact occurs along the path. This can also be beneficial — shared power transfer with proximity to another person wearing a Power-over-Skin transmitter — but improved isolation methods are needed to ensure consistency of power delivery.

8.3 Self-Proximity Modulates Received Power

Power-over-Skin relies on a voltage difference between the body-coupled and ground electrode of the receiver. Consequently, if the body part wearing the transmitter touches both receiver electrodes, no power is received. This effect can be avoided with designs that isolate the receiver ground from accidental body contact. However, if the transmitter and receiver are placed near each other, like our ring joystick where both were placed on the right hand, we found a significant increase in received power when the opposite hand contacted the receiver ground. We believe this is because the other hand is electrically distal, and adds a strong ground coupling to the receiver circuit on contact, which allows higher power transfer. This should allow two-handed applications to access a significantly higher power budget, capable of continuously powering a microcontroller when in contact.

8.4 On-Body Location

Besides on-body distance (results in Figure 9), body location also had a large impact on received power (results in Figure 10). As noted above, any capacitive coupling between the receiver ground and the transmitting body attenuates receiver power. This coupling is inversely proportional to distance, so receivers placed near large planes of the human body (e.g., sternum, neck) cannot access as much power as locations which are further away (e.g., hand, foot). Serendipitously, core body locations can accommodate significantly larger ground and electrode planes than the extremities, however care must to be taken to separate this larger ground plane from accidental self-contact.

8.5 On-Body Backscatter

Backscatter communication offers an alternative to power-hungry wireless protocols like Bluetooth, as they do not require radiating power to send information. While backscatter usually utilizes ambient or transmitted RF energy in the air as its medium, SkinnyPower [23] previously hypothesized that backscatter could be used for devices powered by IBPT, such as Power-over-Skin.

As seen in Figure 11, the presence of one Power-over-Skin receiver on the body is visible to other receivers as a reduction in power. We conducted preliminary experiments showing that a distal receiver also causes a slight reduction in the received power of device placed near the transmitter. Toggling on and off the distal receiver at a rate of 1 MHz, we were able to see the activity from the proximal receiver. Using a single-wire protocol (e.g., NEC protocol for IR remotes), we can transfer information from receiver to transmitter while also powering the receiver over the skin. Any wireless communication can then be offloaded to the transmitter, which can fit a battery and antenna. We believe on-body backscatter is made possible by our improved design — a less efficient receiver would interfere less with other receivers, and therefore be

unable to backscatter data onto the power carrier. To the best of our knowledge, this is the first demonstration of on-body backscatter communication, a technique we hope to mature in future work.

9 CONCLUSION

In this work, we have presented Power-over-Skin, a refinement upon past IBPT systems for energizing battery-free receiver devices worn across the body. This required improvements across every aspect of the system, including circuit design, component choice, and measurement apparatus. We documented over a dozen experiments we ran to inform our system design, which we believe will be invaluable to future researchers. A key result was maintaining power delivery over a diversity of on-body locations and distances in spite of our small receiver board.

This power was enough to run microprocessors and sensors, display output, and perform wireless communication at various worn locations. We believe this capability enables a wide range of new and interesting on-body applications.

ACKNOWLEDGMENTS

We are grateful to Professor Jiamin Li and team for answering our implementation questions, and for granting us permission to incorporate figures from their paper [11]. We would also like to thank Federico Villani for their mentorship in RF simulation.

REFERENCES

[1] Atmel. 1999. https://www.digikey.com/en/products/detail/microchip-technology/ATTINY85-20MU/1245919 Accessed on April 3, 2024.

[2] Minhao Cui, Qing Wang, and Jie Xiong. 2023. Bracelet+: Harvesting the Leaked RF Energy in VLC with Wearable Bracelet Antenna. In *Proceedings of the 20th ACM Conference on Embedded Networked Sensor Systems* (Boston, Massachusetts) *(SenSys '22)*. Association for Computing Machinery, New York, NY, USA, 250–262. https://doi.org/10.1145/3560905.3568526

[3] Paolo de Leva. 1996. Adjustments to Zatsiorsky-Seluyanov's segment inertia parameters. *Journal of Biomechanics* 29, 9 (1996), 1223–1230. https://doi.org/10.1016/0021-9290(95)00178-6

[4] Manoj Gulati, Farshid Salemi Parizi, Eric Whitmire, Sidhant Gupta, Shobha Sundar Ram, Amarjeet Singh, and Shwetak N. Patel. 2018. CapHarvester: A Stick-on Capacitive Energy Harvester Using Stray Electric Field from AC Power Lines. *Proc. ACM Interact. Mob. Wearable Ubiquitous Technol.* 2, 3, Article 110 (sep 2018), 20 pages. https://doi.org/10.1145/3264920

[5] ICNIRP. 2020. Guidelines for Limiting Exposure to Electromagnetic Fields (100 kHz to 300 GHz). *Health Physics* 118, 5 (2020), 483–524.

[6] iFixit. 2022. *AirPods Pro 2 Teardown - Still Completely Unrepairable?* https://www.youtube.com/watch?v=WsxHWKJA7ig

[7] Vikram Iyer, Elyas Bayati, Rajalakshmi Nandakumar, Arka Majumdar, and Shyamnath Gollakota. 2018. Charging a Smartphone Across a Room Using Lasers. *Proc. ACM Interact. Mob. Wearable Ubiquitous Technol.* 1, 4, Article 143 (jan 2018), 21 pages. https://doi.org/10.1145/3161163

[8] Dae-Hyeong Kim, Nanshu Lu, Rui Ma, Yun-Soung Kim, Rak-Hwan Kim, Shuodao Wang, Jian Wu, Sang Min Won, Hu Tao, Ahmad Islam, et al. 2011. Epidermal electronics. *science* 333, 6044 (2011), 838–843.

[9] Konstantin Klamka and Raimund Dachselt. 2021. Bendable Color ePaper Displays for Novel Wearable Applications and Mobile Visualization. In *Adjunct Proceedings of the 34th Annual ACM Symposium on User Interface Software and Technology* (Virtual Event, USA) *(UIST '21 Adjunct)*. Association for Computing Machinery, New York, NY, USA, 6–10. https://doi.org/10.1145/3474349.3480213

[10] LessEMF. 2020. LessEMF. https://lessemf.com/product/stretch-conductive-fabric/ Accessed on April 3, 2024.

[11] Jiamin Li, Yilong Dong, Jeong Hoan Park, and Jerald Yoo. 2021. Body-coupled power transmission and energy harvesting. *Nature Electronics* 4, 7 (2021), 530–538. https://doi.org/10.1038/s41928-021-00592-y

[12] Yichen Li, Tianxing Li, Ruchir A Patel, Xing-Dong Yang, and Xia Zhou. 2018. Self-powered gesture recognition with ambient light. In *Proceedings of the 31st annual ACM symposium on user interface software and technology*. 595–608.

[13] Noor Mohammed, Rui Wang, Robert W. Jackson, Yeonsik Noh, Jeremy Gummeson, and Sunghoon Ivan Lee. 2021. ShaZam: Charge-Free Wearable Devices via Intra-Body Power Transfer from Everyday Objects. *Proc. ACM Interact. Mob. Wearable Ubiquitous Technol.* 5, 2, Article 75 (jun 2021), 25 pages. https://doi.org/10.1145/3463505

[14] Samaneh Movassaghi, Mehran Abolhasan, Justin Lipman, David Smith, and Abbas Jamalipour. 2014. Wireless Body Area Networks: A Survey. *IEEE Communications Surveys & Tutorials* 16, 3 (2014), 1658–1686. https://doi.org/10.1109/SURV.2013.121313.00064

[15] Dairoku Muramatsu and Ken Sasaki. 2021. Input Impedance Analysis of Wearable Antenna and Experimental Study with Real Human Subjects: Differences between Individual Users. *Electronics* 10, 10 (2021). https://doi.org/10.3390/electronics10101152

[16] Simon Olberding, Kian Peen Yeo, Suranga Nanayakkara, and Jurgen Steimle. 2013. AugmentedForearm: exploring the design space of a display-enhanced forearm. In *Proceedings of the 4th Augmented Human International Conference* (Stuttgart, Germany) *(AH '13)*. Association for Computing Machinery, New York, NY, USA, 9–12. https://doi.org/10.1145/2459236.2459239

[17] Gaofeng Pan, Jia Ye, and Zhiguo Ding. 2017. Secure Hybrid VLC-RF Systems With Light Energy Harvesting. *IEEE Transactions on Communications* 65, 10 (2017), 4348–4359. https://doi.org/10.1109/TCOMM.2017.2709314

[18] PowerCast. 2020. https://www.powercastco.com/ Accessed on April 3, 2024.

[19] Tamer Rakia, Hong-Chuan Yang, Fayez Gebali, and Mohamed-Slim Alouini. 2016. Optimal Design of Dual-Hop VLC/RF Communication System With Energy Harvesting. *IEEE Communications Letters* 20, 10 (2016), 1979–1982. https://doi.org/10.1109/LCOMM.2016.2595561

[20] Harilaos G Sandalidis, Alexander Vavoulas, Theodoros A Tsiftsis, and Nicholas Vaiopoulos. 2017. Illumination, data transmission, and energy harvesting: the threefold advantage of VLC. *Applied optics* 56, 12 (2017), 3421–3427.

[21] Takuya Sasatani, Alanson P. Sample, and Yoshihiro Kawahara. 2021. Room-scale magnetoquasistatic wireless power transfer using a cavity-based multimode resonator. *Nature Electronics* 4, 9 (01 Sep 2021), 689–697. https://doi.org/10.1038/s41928-021-00636-3

[22] Seeed Studio. 2023. XIAO nRF52840. https://www.seeedstudio.com/Seeed-XIAO-BLE-nRF52840-p-5201.html.

[23] Rishi Shukla, Neev Kiran, Rui Wang, Jeremy Gummeson, and Sunghoon Ivan Lee. 2019. SkinnyPower: enabling batteryless wearable sensors via intra-body power transfer. In *Proceedings of the 17th Conference on Embedded Networked Sensor Systems* (New York, New York) *(SenSys '19)*. Association for Computing Machinery, New York, NY, USA, 68–82. https://doi.org/10.1145/3356250.3360034

[24] Saichon Sriphan and Naratip Vittayakorn. 2022. Hybrid piezoelectric-triboelectric nanogenerators for flexible electronics: Recent advances and perspectives. *Journal of Science: Advanced Materials and Devices* 7, 3 (2022), 100461. https://doi.org/10.1016/j.jsamd.2022.100461

[25] Kyung Ho Sun, Jae Eun Kim, Jedo Kim, and Kyungjun Song. 2017. Sound energy harvesting using a doubly coiled-up acoustic metamaterial cavity. *Smart materials and Structures* 26, 7 (2017), 075011.

[26] Shan-Yuan Teng, K. D. Wu, Jacqueline Chen, and Pedro Lopes. 2022. Prolonging VR Haptic Experiences by Harvesting Kinetic Energy from the User. In *Proceedings of the 35th Annual ACM Symposium on User Interface Software and Technology* (Bend, OR, USA) *(UIST '22)*. Association for Computing Machinery, New York, NY, USA, Article 39, 18 pages. https://doi.org/10.1145/3526113.3545635

[27] Virag Varga, Marc Wyss, Gergely Vakulya, Alanson Sample, and Thomas R. Gross. 2018. Designing Groundless Body Channel Communication Systems: Performance and Implications. In *Proceedings of the 31st Annual ACM Symposium on User Interface Software and Technology* (Berlin, Germany) *(UIST '18)*. Association for Computing Machinery, New York, NY, USA, 683–695. https://doi.org/10.1145/3242587.3242622

[28] Benjamin Vigoda and Neil Gershenfeld. 1999. TouchTags: using touch to retrieve information stored in a physical object. In *CHI '99 Extended Abstracts on Human Factors in Computing Systems* (Pittsburgh, Pennsylvania) *(CHI EA '99)*. Association for Computing Machinery, New York, NY, USA, 264–265. https://doi.org/10.1145/632716.632879

[29] Edward J. Wang, Manuja Sharma, Yiran Zhao, and Shwetak N. Patel. 2018. CASPER: capacitive serendipitous power transfer for through-body charging of multiple wearable devices. In *Proceedings of the 2018 ACM International Symposium on Wearable Computers* (Singapore, Singapore) *(ISWC '18)*. Association for Computing Machinery, New York, NY, USA, 188–195. https://doi.org/10.1145/3267242.3267254

[30] Martin Weigel, Aditya Shekhar Nittala, Alex Olwal, and Jürgen Steimle. 2017. SkinMarks: Enabling Interactions on Body Landmarks Using Conformal Skin Electronics. In *Proceedings of the 2017 CHI Conference on Human Factors in Computing Systems* (Denver, Colorado, USA) *(CHI '17)*. Association for Computing Machinery, New York, NY, USA, 3095–3105. https://doi.org/10.1145/3025453.3025704

[31] Paul Worgan and Mike Fraser. 2016. Garment level power distribution for wearables using inductive power transfer. In *2016 9th International Conference on Human System Interactions (HSI)*. 277–283. https://doi.org/10.1109/HSI.2016.7529644

[32] Joanne E. Zucco and Bruce H. Thomas. 2016. Design Guidelines for Wearable Pointing Devices. *Frontiers in ICT* 3 (2016). https://doi.org/10.3389/fict.2016.00013